

## EXPERIMENTAL RESULTS ON POLARIZED NUCLEON STRUCTURE FUNCTIONS\* \*\*

EWA RONDIO

for the Spin Muon Collaboration at CERN

Andrzej Soltan Institute for Nuclear Studies,  
Hoża 69, 00-681 Warsaw, Poland  
e-mail: ewar@fuw.edu.pl

*(Received July 1, 1998)*

Experimental results of deep inelastic scattering of polarized leptons from polarized target nucleons are reviewed. Accurate values of the spin dependent structure function  $g_1(x)$  were obtained in those experiments covering a large kinematic range. The combination of all experimental results confirms the validity of the Bjorken sum rule.

PACS numbers: 12.38.Qk, 12.38.-t, 13.60.-r, 11.55.Hx

### 1. Introduction

During the last decade several experiments of polarized deep inelastic lepton scattering were completed. The main issues were the earlier observed deviation from the Ellis-Jaffe sum rule [1,2] and the validity of the Bjorken sum rule [3]. Both at SLAC and at CERN experimental groups collected vast amounts of data within the limits of their experimental set-ups. These experiments finished data taking and most of the results are already available. Also the semi-inclusive measurements bring information about the spin structure of the nucleon. These are available from the SMC experiment at CERN and from Hermes at DESY. The Hermes experiment is still taking data and more information from it is expected.

The high quality data on the spin dependent structure function  $g_1(x, Q^2)$  from all these experiments, in overlapping kinematic domains, allowed for a QCD analysis and the extraction of polarized parton distributions. The

---

\* Presented at the Meson'98 and Conference on the Structure of Meson, Baryon and Nuclei, Cracow, Poland, May 26–June 2, 1998.

\*\* This work was supported by the research grant KBN no.2/P03B/081/14.

richness of the information which can be obtained from a QCD analysis of  $g_1$  is in principle larger than that of the structure function  $F_2$ . However, the experimental data on  $g_1$  is yet more limited in statistical accuracy and kinematic range. It should be part of a future program for spin effects in particle physics to determine  $g_1$  with improved accuracy over a larger  $x$  and  $Q^2$  range, if possible, at the HERA collider.

## 2. How does the DIS “see” the quark spin

The spin-dependent part of the cross section can be written in terms of two structure functions  $g_1$  and  $g_2$  which describe the interaction of lepton and hadron currents. Let's consider an interaction in which spins of leptons and nucleons in the target are parallel. We can relate measured cross section to the quark spin orientation. Since a virtual photon can only be absorbed when its spin is anti parallel to the quark spin we can consider two situations shown in Fig. 1 corresponding to  $\sigma_{1/2}$  and  $\sigma_{3/2}$ , where the index gives a total spin of the virtual gamma-nucleon system.

$$A_1 = \frac{\sigma_{1/2} - \sigma_{3/2}}{\sigma_{1/2} + \sigma_{3/2}} = \frac{g_1 - \gamma^2 g_2}{F_1}. \quad (1)$$

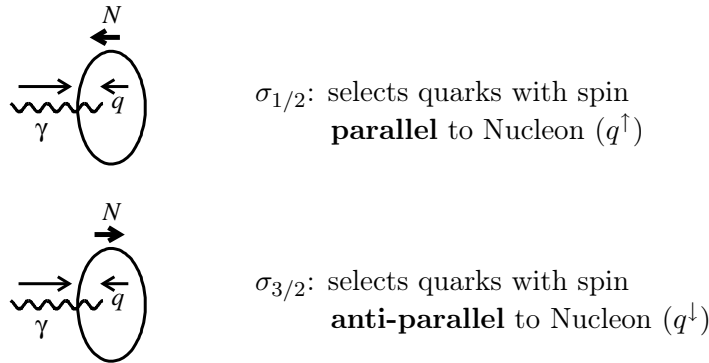


Fig. 1. An illustration for quark parton model interpretation of the cross sections with the same (3/2) and opposite (1/2) virtual  $\gamma$  and nucleon spin orientations.

In order to conserve angular momentum, a virtual photon with helicity  $+1$  or  $-1$  can only be absorbed by a quark with a spin projection of  $-1/2$  or  $+1/2$ , respectively, if the quarks have no orbital angular momentum. Hence,  $A_1$  and  $g_1$  contain information on the quark spin orientations with respect to the proton spin direction.

### 3. Measurements of asymmetry $A_1$

Experiments of deep inelastic lepton-nucleon scattering with polarized beams and polarized targets are summarized in Table I. The kinematic acceptances of SLAC and CERN experiments for  $Q^2 \geq 1 \text{ GeV}^2$  are shown in Fig. 2. The higher energy of the electron or muon beam allows measurements at smaller values of the Bjorken scaling variable  $x$ .

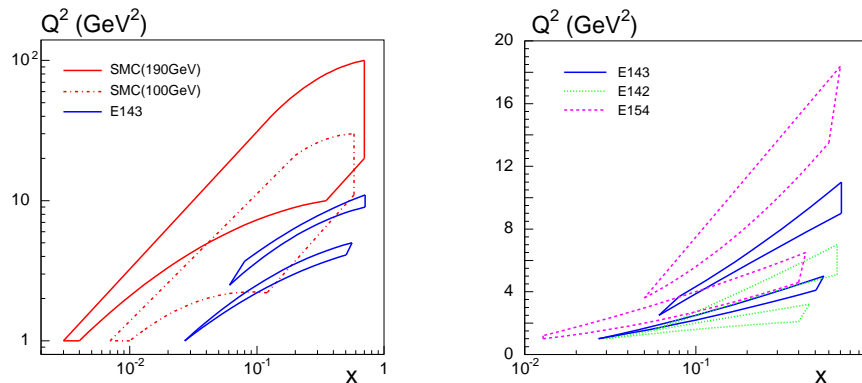


Fig. 2. Kinematic ranges in  $x$  and  $Q^2$  covered by the SMC and recent SLAC experiments with the data with  $Q^2 > 1 \text{ GeV}^2$ .

TABLE I

Comparison of the kinematic ranges in  $x$  and  $Q^2$  covered by experiments measuring  $g_1$ .

Experiment	beam	$E$ (GeV)	smallest $x$ $Q^2 > 1 \text{ GeV}^2$	average $Q^2$ ( $\text{GeV}^2$ )	target nucleon
E80/130	$e^-$	23	0.10	4	$p$
EMC	$\mu^+$	100–200	0.01	10.7	$p$
SMC	$\mu^+$	100–190	0.003	10	$p, d$
E142	$e^-$	19–25	0.03	2	$n$
E143	$e^-$	10–29	0.029	3	$p, d$
E154	$e^-$	48.3	0.014	5	$n$
E155	$e^-$	48.3	0.014	5	$p, d$
HERMES	$e^+$	27.5	0.023	2.3	$n, p$

Measured count rate asymmetries for opposite longitudinal beam or target polarizations were used to determine the virtual photon asymmetry  $A_1(x)$ , where the count rate

$$N = n\phi a\bar{\sigma}\{1 - fDP_bP_t(A_1 + \eta A_2)\} \quad (2)$$

depends on the target density per  $\text{cm}^2$ ,  $n$ , the beam flux  $\phi$ , the detector acceptance  $a$ , the unpolarized cross section  $\bar{\sigma}$ , the dilution factor  $f$ , the depolarization factor  $D$ , the beam polarization  $P_b$ , the target polarization  $P_t$ , and the spin asymmetry  $A_1$ . The contribution from  $A_2$  is small as the kinematic factor  $\eta$  is small and the asymmetry  $A_2$  was measured [4] to be consistent with zero in most of the kinematic range of the measurements discussed here. The uncertainties due to  $n$ ,  $\phi$ ,  $a$  and  $\bar{\sigma}$  cancelled to a large extent by the way the experiments were carried out and analyzed.

The world data for  $Q^2 \geq 1 \text{ GeV}^2$  on the spin asymmetries  $A_1(x)$  presently published are shown in Fig. 3. The data were published by EMC [1], SMC [5], E142 [6], E143 [7], E154 [8], and HERMES [9]. A very precise data from E155 are available as preliminary. These data and more data from HERMES are expected to be published soon.

At the lower values of  $x$  there are measurements from SMC, see Fig. 4. These data cover  $Q^2$  range down to  $Q^2 = 0.01 \text{ GeV}^2$  at the lowest  $x$ .

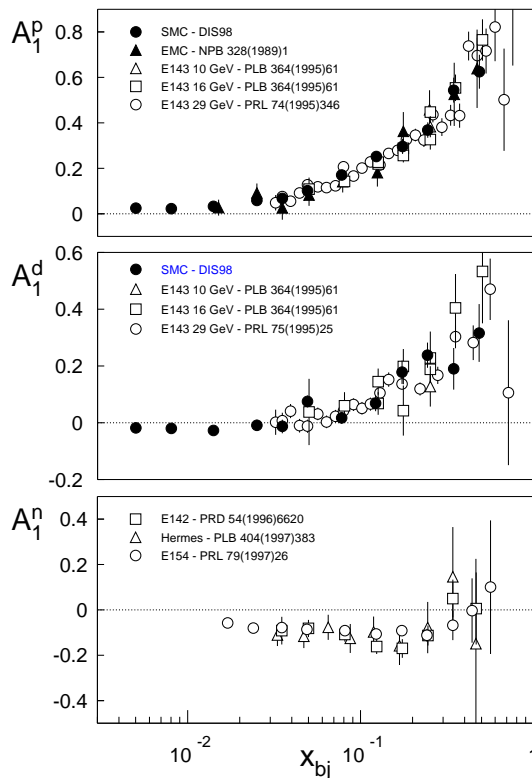


Fig. 3. World data on  $A_1^p$ ,  $A_1^d$  and  $A_1^n$  if  $Q^2 \geq 1 \text{ GeV}^2$  is required. The errors are statistical. These data were used in the QCD analysis discussed in the text.

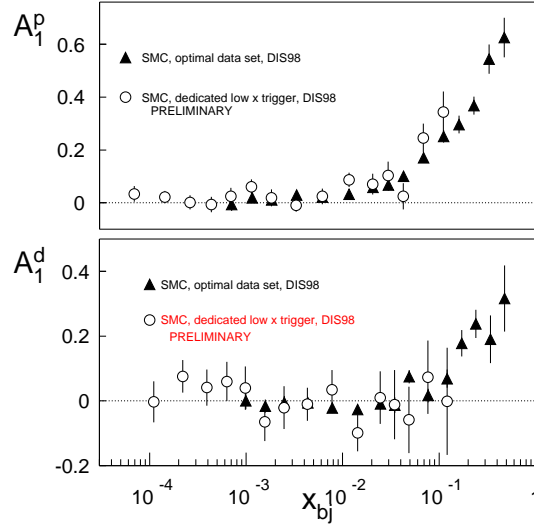


Fig. 4. The spin asymmetry  $A_1$  at low  $x$  and low  $Q^2$  measured by SMC. The optimal data set with  $Q^2 > 0.2\text{GeV}^2$  and the very low  $x$  data, which are still preliminary, obtained with dedicated low  $x$  trigger with the hadron requirement. This allows access to the kinematic region where elastic scattering of muons or atomic electrons would be dominant for inclusive measurement.

#### 4. Evaluation of $g_1$ and tests of sum rules

The spin dependent structure function  $g_1^p(x, Q^2)$  is determined from the measured spin asymmetries  $A_1(x, Q^2)$  and parametrizations of the unpolarized structure functions  $F_2$  and  $R$ . Recently a next-to-leading order QCD analysis of the world data (all data shown in Fig. 3) was performed [10]. The distributions for singlet quarks and gluons obtained in this analysis is shown in Fig. 5. The results of this analysis were used to calculate the first moments

$$\Gamma_1 = \int_0^1 g_1(x) dx$$

for the proton, deuteron and neutron at a fixed value of  $Q_0^2$ . The  $Q_0^2 = 5\text{ GeV}^2$  was chosen as it is close to the average  $Q^2$  of the data. The results of the QCD fit were used for the extrapolation of  $g_1$  from measured  $Q^2$  to  $Q_0^2 = 5\text{ GeV}^2$  and also for the extrapolation to unmeasured regions towards  $x = 0$  and  $x = 1$ . The results obtained for the first moments of  $g_1$ :  $\Gamma_1^p = 0.121 \pm 0.003(\text{stat.}) \pm 0.005(\text{syst.}) \pm 0.017(\text{QCD})$ ,  $\Gamma_1^d = 0.021 \pm 0.004 \pm 0.003 \pm 0.016$  and  $\Gamma_1^n = -0.075 \pm 0.007 \pm 0.005 \pm 0.019$  are all significantly lower than the Ellis–Jaffe sum rule predictions, as it is shown in Fig. 6 where they are

shown as bands of one standard deviation around their central values. The errors are dominated by the uncertainty on the low  $x$  extrapolation.

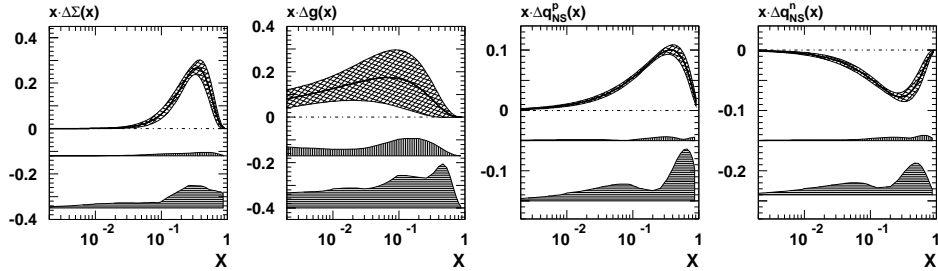


Fig. 5. The polarized parton distribution functions determined from pQCD analysis at  $Q^2 = 1\text{GeV}^2$ . Their statistical uncertainty is shown as a band with crossed hatch and two bands indicate experimental (upper) and the theoretical (lower) uncertainties.

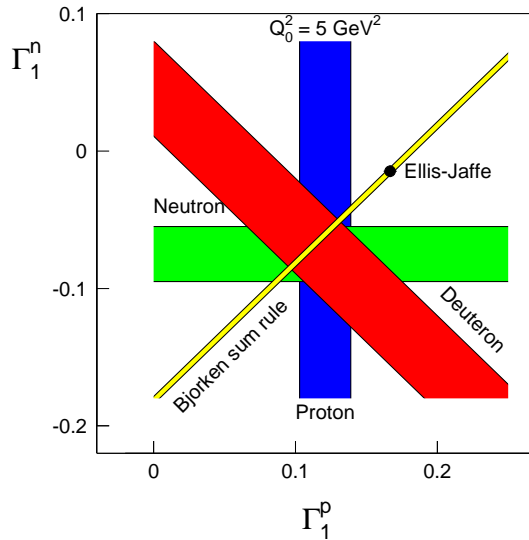


Fig. 6. The first moments of  $g_1^{p,d,n}(x)$  at  $Q_0^2 = 5\text{ GeV}^2$ , as given in the text, compared with the Bjorken, and Ellis-Jaffe predictions.

From Fig. 6 one can also see that all the data are consistent with the validity of the Bjorken sum rule, predicting  $\Gamma_1^p - \Gamma_1^n = 0.181 \pm 0.003$  at  $Q_0^2 = 5\text{ GeV}^2$ . In the QCD fit the test of Bjorken sum rule is done by using as an extra parameter the axial vector coupling constant  $g_A/g_V$ . The result obtained corresponds to  $\Gamma_1^p - \Gamma_1^n = 0.174 \pm 0.24/0.12$  at this  $Q^2$ . The value of  $\Gamma_1^p - \Gamma_1^n$  was also calculated from the direct integration of the non-singlet structure function  $g_1^{\text{NS}}(x, Q^2)$ . Fig. 7 shows  $xg_1^{\text{NS}}(x, Q^2)$

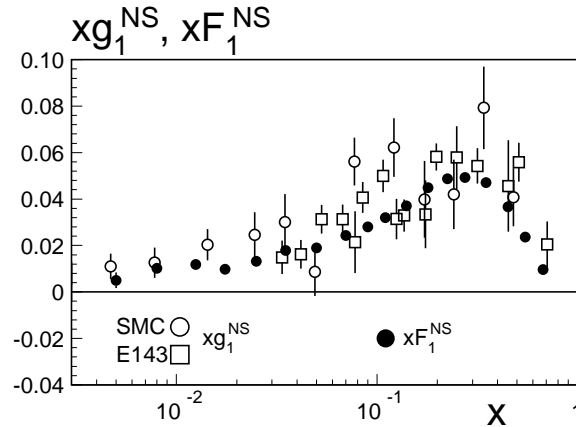


Fig. 7. The non-singlet functions  $xg_1^{\text{NS}}$  and  $xF_1^{\text{NS}}$ . Both functions are presented at the measured  $Q^2$  of the experiments. The errors are statistical only.

calculated for SMC and E143 experiments as a function of  $x$  at average value of  $Q^2$  of the measurement. The changes of  $g_1^{\text{NS}}$  due to the  $Q^2$  evolution are small. For SMC data at  $Q^2 = 10 \text{ GeV}^2$  from the integrating  $g_1^{\text{NS}}$  we obtain  $\Gamma_1^p - \Gamma_1^n = 0.198 \pm 0.023$ , which should be compared with theoretical prediction of  $0.186 \pm 0.003$  at this  $Q^2$ .

## 5. Polarized quark distributions

Semi-inclusive spin asymmetries for positively and negatively charged hadrons from polarized protons and deuterons and  $^3\text{He}$  were analyzed to determine the polarized valence quark distributions  $\Delta u_v(x)$  and  $\Delta d_v(x)$ , as well as the polarized sea quark distribution  $\Delta \bar{q}(x)$ . In Fig. 8 these distributions published by SMC experiment [11] are compared with preliminary ones from HERMES [12]. The results are consistent in the overlapping  $x$  range. The polarization of the  $u_v$  quarks was found to be positive and to increase with  $x$ , while for the  $d_v$  quarks it was found to be negative. For the sea quarks the observed polarization was consistent with zero with high accuracy at small  $x$ . From the SMC data the first moments of the polarized quark distributions were  $\Delta u_v = 0.77 \pm 0.10 \pm 0.08$ ,  $\Delta d_v = -0.52 \pm 0.14 \pm 0.09$ , and  $\Delta \bar{q} = 0.010 \pm 0.04 \pm 0.03$ .

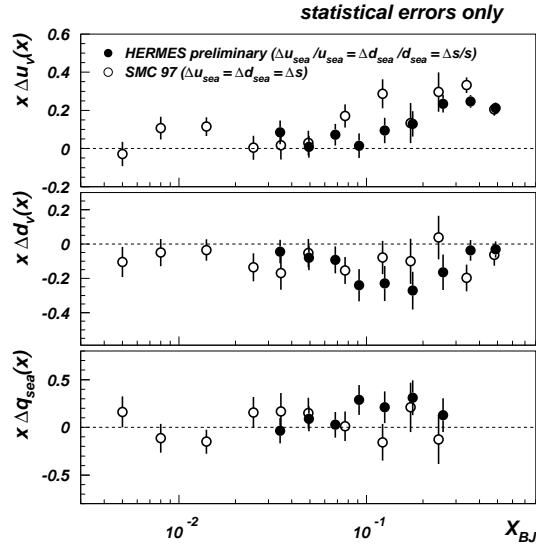


Fig. 8. Flavour separated polarized quark distributions  $x\Delta q(x)$ . The open circles results from SMC experiment, close circles - preliminary results from HERMES. The errors shown are only statistical. Systematic uncertainty estimated in SMC experiment are smaller than statistical ones.

## 6. Conclusions

The presented data sets of  $A_1$  cover a substantial range in  $x$ . The use of polarized  $^3\text{He}$  target in the E142 and E154 experiments at SLAC and by HERMES at DESY provides direct measurements of  $g_1^n$  which are in good agreement with the combined proton and deuteron data.

The NLO-QCD analysis of all available data was performed and the results were used to extrapolated measured polarized structure functions  $g_1$ 's to common value of  $Q^2$  and to estimate contributions to the first moments from the unmeasured regions. The results for the first moments  $I_1^{p,d,n}$  confirm the validity of the Bjorken sum rule with an uncertainty of about 10 percent. The violation of the Ellis-Jaffe sum rule is clearly demonstrated and indicates either a large negative polarization of strange quarks in the nucleon or a large positive gluon spin contribution to the nucleon spin at a relatively low  $Q^2$  scale.

Polarization distributions for up and down valence quarks are determined from semi-inclusive asymmetries in the framework of the quark parton model. Positive polarization of up valence quarks and negative polarization of down valence quarks in the proton are demonstrated, together with vanishing polarization of up and down sea quarks. More data on semi-inclusive

neutron asymmetries are needed to improve the accuracy of the down valence quark polarization distribution and to test isospin symmetry of polarized parton distributions. The main purpose of the polarized semi-inclusive lepton nucleon scattering experiments of HERMES and COMPASS will be a direct measurement of the gluon polarization.

## REFERENCES

- [1] J. Ashman *et al.*, *Phys. Lett.* **B206**, 364 (1988); *Nucl. Phys.* **B328**, 1 (1989).
- [2] J. Ellis, R.L. Jaffe, *Phys. Rev.* **D9**, 1444 (1974); **D10**, 1669 (1974).
- [3] J.D. Bjorken, *Phys. Rev.* **148**, 1467 (1966); **D1**, 1376 (1970).
- [4] SMC, D.Adams *et al.*, *Phys. Lett.* **B336**, 125 (1994); E143, K. Abe *et al.*, *Phys. Rev. Lett.* **76**, 587 (1996).
- [5] SMC, B. Adeva *et al.*, accepted in *Phys. Rev.* **D**; J. Cranshaw, presentation at DIS98 Conference, Brussel 1998.
- [6] E142, D.L. Anthony *et al.*, *Phys. Rev. Lett.* **71**, 959 (1993); *Phys. Rev.* **D54**, 6620 (1996).
- [7] E143, K. Abe *et al.*, *Phys. Rev. Lett.* **74**, 346 (1995); **75**, 25 (1995); **76**, 587 (1996); *Phys. Lett.* **B364**, 61 (1995).
- [8] E154, K. Abe *et al.*, *Phys. Rev. Lett.* **79**, 26 (1997).
- [9] HERMES, K. Ackerstaff *et al.*, *Phys. Lett.* **B404**, 383 (1997).
- [10] SMC, B. Adeva *et al.*, accepted in *Phys. Rev.* **D**; E.P. Sichtermann, presentation at DIS98 Conference, Brussel 1998.
- [11] SMC, D. Adams *et al.*, *Phys. Lett.* **B329**, 399 (1994); CERN-PPE/97-147, to be publ. in *Phys. Lett.* **B**.
- [12] HERMES, K. Rith, presentation at the DIS98 Conference, Brussel, 1998.